4.21 THE ROLE OF TOTAL LIGHTNING IN THUNDERSTORM NOWCASTING

Martin J. Murphy* and Nicholas Demetriades
Vaisala Inc.
Tucson, Arizona, USA

1. INTRODUCTION

The objective of this paper is to show that observations of total lightning activity provide significant benefits for thunderstorm nowcasting problems. For the purposes of this paper, the term "total lightning activity" refers to the combination of in-cloud (IC) and cloud-to-ground (CG) lightning flashes. We focus on a couple of key nowcasting issues in this paper: (1) thunderstorm growth and decay, (2) the CG lightning threat to life and property, and (3) timely notice of the threat of severe weather.

To be effective, systems that observe total lightning activity must be capable of detecting the vast majority of both IC and CG flashes and must also differentiate between the two. Observations from a combination of systems are discussed in this paper. CG flash observations are taken from the U.S. National Lightning Detection Network (NLDN; Cummins et al. 1998). Observations of cloud lightning flashes that have no CG component, as well as the in-cloud components of CG flashes, are provided by ground-based lightning mapping systems that operate in the VHF. Either interferometric or time-of-arrival techniques may be employed to detect in-cloud lightning activity in the VHF band (Mazur et al. 1997). In this paper, VHF lightning information is provided either by the LDAR II time-of-arrival network operated by Vaisala in the vicinity of Dallas, Texas (Demetriades *et al.* 2002) or by a network of SAFIR interferometric sensors in the same area (Richard, 1991). Where needed, radar information is taken from the National Weather Service S-band Dopper radar located to the south of Fort Worth, Texas.

The choice of the Dallas-Fort Worth, Texas, area (hereafter, DFW) for the cases discussed in this paper has special significance because of an ongoing collaboration between the National Weather Service (NWS), NASA, Vaisala, and others to integrate Vaisala total lightning observations into the NWS Fort Worth office. Total lightning data were first delivered to an NWS office through the efforts of the NASA SPoRT program (Goodman et al. 2004), and this program was expanded to include Vaisala and the Fort Worth NWS office in 2004.

Corresponding author: Martin Murphy, Vaisala Inc., 2705 E. Medina, Tucson AZ 85706 USA, martin.murphy@vaisala.com

2. THUNDERSTORM GROWTH AND DECAY

Lightning activity in developing thunderstorms typically begins with IC flashes (Williams et al. 1989), and in the DFW region, IC flashes outnumber CG flashes by about a factor of 4 (Boccippio et al. 2001). Together, these imply that total lightning detection provides the earliest indication of thunderstorm development, and better resolution of the phase of thunderstorm life cycle. Figure 1 shows the total lightning observations for an isolated thundercloud near DFW on 27 June 2001. Three observations from the radar are also shown: echo top altitude, average reflectivity within 5 km of the cell, and maximum vertically integrated liquid. The electrically active phase of this cell exhibited two peaks in total flash rate. Most of the relative scarce CG activity was associated with the second peak. The only radar parameter that correlated reasonably well was the maximum VIL, although the radar time resolution of 5 minutes is poorer than that of the lightning activity. Neither echo altitude nor average low-level reflectivity indicated when the cell had developed sufficiently to produce lightning.

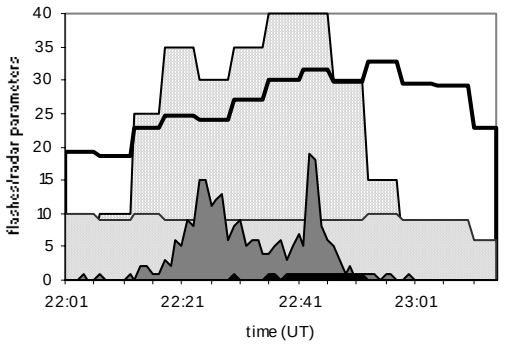

Fig. 1. Time series of lightning and radar observations of an isolated cell. Thick solid line shows average low-level reflectivity (in dBZ) within the cell. Stippled area: maximum vertically integrated liquid (kg/m2). Hatched area: maximum echo altitude (km). Gray solid fill area: total flashes per minute. Black solid fill area: negative CG flashes per minute.

Time-of-arrival systems such as LDAR II also provide the altitudes of the VHF radiation detected. The maximum altitude of radiation

events is also linked to the growth and decay of storms, as shown by Fig. 2, which compares the upper altitude (95th percentile) of lightning activity and the total flash rate for an isolated storm on 25 May 2002. The graph starts a few minutes after the initial lightning flash in the storm because a certain minimum rate of VHF radiation is required in order to determine a meaningful value of the 95th percentile altitude. However, after that time, we note a good correlation between the flash rate and upper altitude of lightning activity, particularly during the decay phase of the storm after 05:00.

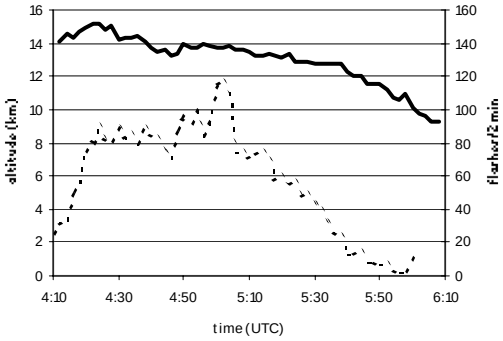

Fig. 2. Time series of the uppermost altitude of lightning activity (solid line) and flash rate (dotted line) for storm on 25 May 2002.

3. CG LIGHTNING THREAT

Total lightning observations can be used in combination with cloud-to-ground (CG) lightning detection data to reduce the rate of failures to warn (FTW) significantly in difficult CG lightning warning situations The reduction in FTW is much more significant than the increase in total warning duration. When automated CG lightning warnings are based primarily on CG lightning detection data, they often expire too soon during situations of low lightning flash rate and density, such as under the stratiform regions of mesoscale convective systems (MCSs). Subsequent CG flashes then sometimes occur after the automated warnings expire. These cases amount to failures to warn and can be a serious hazard to people who return to outdoor activity when automated warnings expire.

The improved method discussed by Murphy and Holle (2005) involves adding total lightning and radar, or just total lightning, to the CG detection data to indicate lightning threat and hopefully reduce the FTW. Fig. 3 illustrates the full method that involves total lightning and radar data. There are four levels of "alert" and a fifth level that denotes where CG lightning is currently occurring. The four levels of alert and their corresponding color levels in Fig. 3 are as follows: (1) GREEN: reflectivity above a minimum level (typically 10 dBZ) without lightning, (2) CYAN: cloud lightning without reflectivity, (3) BLUE: cloud lightning with reflectivity below a threshold, and (4) YELLOW: cloud lightning with reflectivity above the same threshold. Red areas in Fig. 3 show where CG flashes are occurring. A similar, simpler method is also discussed by Murphy and Holle (2005) that omits the radar information and just uses two levels (1: IC activity but no CG, 2: CG occurring). By applying the total lightning-based methods to MCSs with extensive stratiform regions, Murphy and Holle were able to show a reduction of about a factor of 4 in the rate of failures to warn relative to a warning method based on CG lightning data alone. This significant reduction was realized with the total lightning observations regardless of the presence of the radar data. The radar observations served to keep the total increase in warning duration under control; total warning duration only increased by 18% for the five-level total lightning-based method relative to the CG-only method.

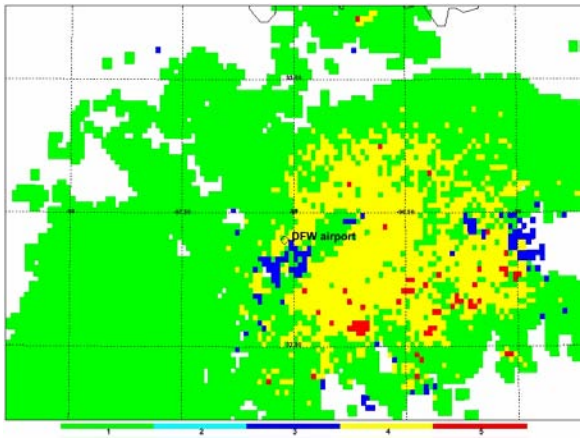

Fig. 3. Example of total lightning and radar-based graphic for CG lightning warnings. See text for description of color scale.

4. SEVERE WEATHER OBSERVATIONS

A couple of cases of severe weather were identified by the Fort Worth NWS office, and these serve to illustrate how total lightning observations can be used. Figures 4a-4d show a sequence of lightning activity (measured by the "flash extent density" or FED, Lojou and Cummins, 2005) images on 10 April 2005. This sequence shows a rapid increase in the intensity of lightning activity in the core of the storm followed by a rapid increase in the area of the

storm covered by the highest lightning activity levels. In addition, the last two images in the sequence show a change in shape of the storm to include a slight notch on the southwestern (trailing) side of the cell. The rapid increase in lightning activity and areal coverage and the change in cell shape preceded the production of 2.5-cm hail and 125 km/hr wind at the surface, with a lead time of about 5 minutes.

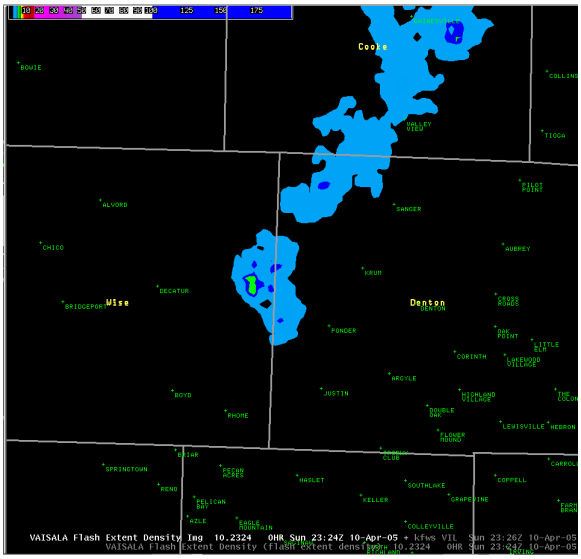

Fig. 4a. Lightning activity (flash extent density) at 2324 UTC on 10 April 2005. White lines are boundaries of counties in the state of Texas. DFW International Airport is located near the lower right corner of the map area.

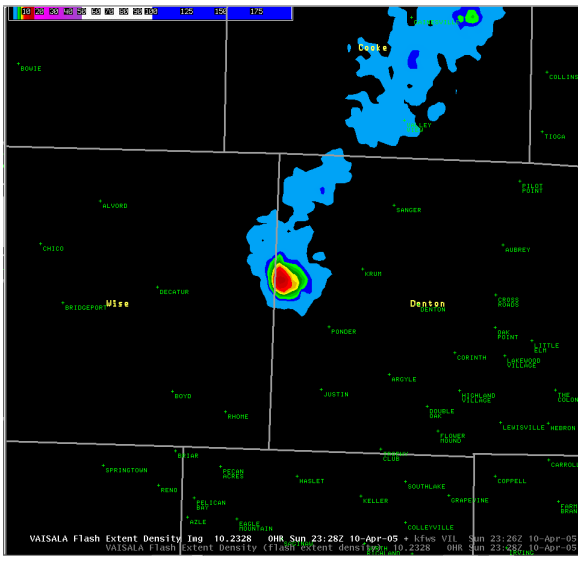

Fig. 4b. As in 4a but at 2328 UTC.

Another storm on 25 April 2005 produced a tornado to the south of the DFW International Airport. Figures 5a-5c show the total lightning flash extent density over a 6-minute period. During this time, the maximum lightning activity increases and the lightning activity begins to develop toward the south (Fig. 5b). This is the first sign that the main cell is beginning to turn to the right of its former path. Eventually the highest FED values are found at the southern end of the cell (Fig. 5c). This coincides with the detection of a bounded weak echo region at middle levels by the radar, as shown in the upper right panel of Fig. 6. The lightning observations provided the first indication of the turning and strengthening of the cell, which produced a tornado about 20 minutes later.

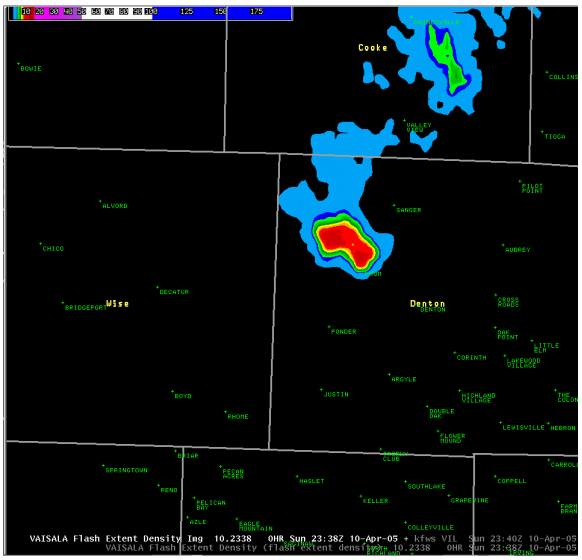

Fig. 4c. As in 4b but at 2338 UTC.

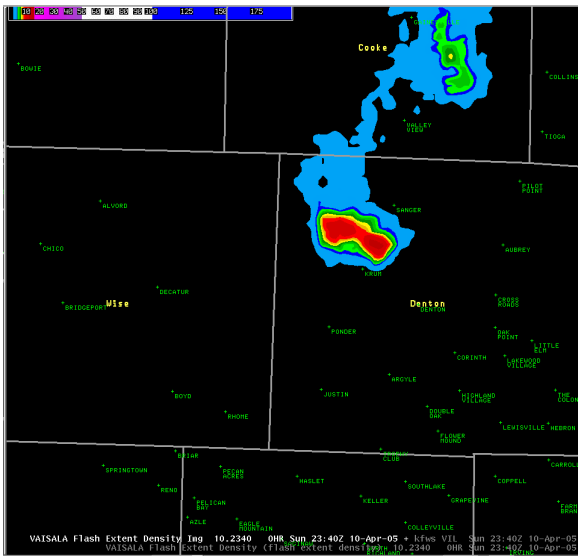

Fig. 4d. As in 4c but at 2340 UTC.

REFERENCES

Boccippio, D.J., K.L. Cummins, H.J. Christian, and S.J. Goodman, 2001: Combined

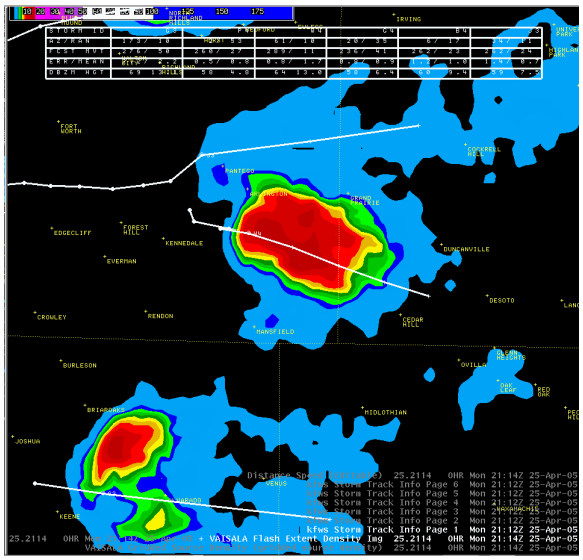

Fig. 5a. Lightning flash extent density at 2114 UTC on 25 April 2005. The storm of interest is in the center of the image.

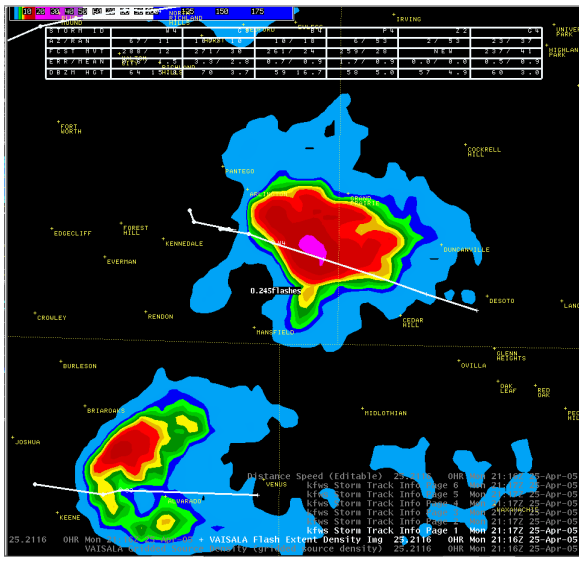

Fig. 5b. As in 5a but at 2116 UTC.

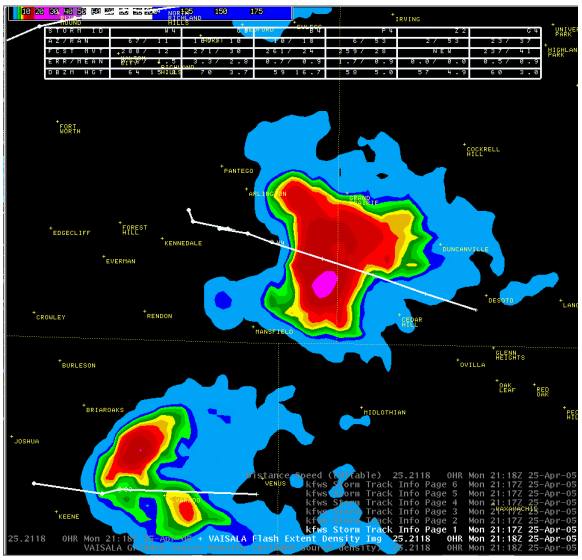

Fig. 5c. As in 5b but at 2118 UTC.

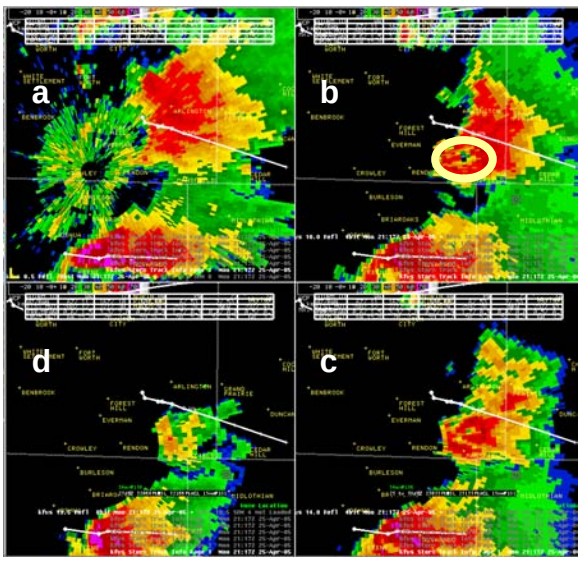

Fig. 6. Series of radar data from a volume scan started at 2117 UTC on 25 April 2005. The approximate altitude of the radar beam within the storm of interest for each panel are (a) 0.2 km, (b) 3.0 km, (c) 4.3 km, and (d) 5.8 km. A bounded weak echo region (circled in yellow) is seen in panel (b).

satellite- and surface-based estimation of the intracloud–cloud-to-ground lightning ratio over the continental United States. *Mon. Wea. Rev.*, **129**, 108-122.

Cummins, K.L., M.J. Murphy, E.A. Bardo, W.L. Hiscox, R.B. Pyle, and A.E. Pifer, 1998: A combined TOA/MDF technology upgrade of the U.S. National Lightning Detection Network. *J. Geophys. Res.*, **103**, 9035-9044.

Demetriades, N.W.S., M.J. Murphy, and K.L. Cummins, 2002: Early results from the Global Atmospherics, Inc., Dallas-Fort Worth Lightning Detection and Ranging (LDAR II) research network. 6th Conf. on Integrated Observing Systems, Amer. Meteorol. Soc., Orlando, FL, 202-209.

Goodman, S.J., W.M. Lapenta, G.J. Jedlovec, J.C. Dodge, and J.T. Bradshaw, 2004: The Short-term Prediction Research and Transition (SPoRT) center: A collaborative model for accelerating research into operations. 20th Intl. Conf. on IIPS for Meteorology, Oceanography, and Hydrology, Amer. Meteorol. Soc., Seattle, WA, paper P1.34 (CD-ROM).

Lojou, J-Y. and K.L. Cummins, 2005: On the representation of two- and three-

dimensional total lightning information. Conf. on the Meteorological Applications of Lightning Data, Amer. Meteorol. Soc., San Diego, CA, paper 2.4 (CD-ROM)

Mazur, V., E. Williams, R. Boldi, L. Maier, and D.E. Proctor, 1997: Initial comparison of lightning mapping with operational time-of-arrival and interferometric systems. *J. Geophys. Res.*, **102**, 11071-11085.

Murphy, M.J. and R.L. Holle, 2005: A warning method for the risk of cloud-to-ground lightning based on total lightning and radar information. Intl. Conf. on Lightning and Static Elec., The Boeing Co., Seattle, WA.

Richard, P., 1991: Localization of atmospheric discharges, a new way for severe weather nowcasting. 25th Intl. Conf. on Radar Meteorology, Amer. Meteorol. Soc., Paris, 911-915.

Williams, E.R., M.E. Weber, and R.E. Orville, 1989: The relationship between lightning type and convective state of thunderclouds. *J. Geophys. Res.*, **94**, 13213-13220.